WL-TR-92-7016

4.5 Micron Laser Source

Dr. M. A. Acharekar
Mr. J. Montgomery

Schwartz Electro-Optics, Inc.
3404 North Orange Blossom Trail
Orlando FL 32804

JUNE 1992

FINAL REPORT FOR PERIOD MARCH - OCTOBER 1991

WRIGHT LABORATORY, ARMAMENT DIRECTORATE
Air Force Systems Command ▮ United States Air Force ▮ Eglin Air Force Base

NOTICE

When Government drawings, specifications, or other data are used for any purpose other than in connection with a definitely Government-related procurement, the United States Government incurs no responsibility or any obligation whatsoever. The fact that the Government may have formulated or in any way supplied the said drawings, specifications, or other data, is not to be regarded by implication, or otherwise as in any manner construed, as licensing the holder, or any other person or corporation; or as conveying any rights or permission to manufacture, use, or sell any patented invention that may in any way be related thereto.

This technical report has been reviewed and is approved for publication.

The Public Affairs Office has reviewed this report, and it is releasable to the National Technical Information Service (NTIS), where it will be availabe to the general public, including foreign nationals.

FOR THE COMMANDER

George F. Kirby

GEORGE F. KIRBY
Chief, Analysis and Strategic Defense Division

Even though this report may contain special release rights held by the controlling office, please do not request copies from the Wright Laboratory, Armament Directorate. If you qualify as a recipient, release approval will be obtained from the originating activity by DTIC. Address your request for additional copies to:

Defense Technical Information Center
Cameron Station
Alexandria VA 22304-6145

If your address has changed, if you wish to be removed from our mailing list, or if your organization no longer employs the addressee, please notify WL/MN SI, Eglin AFB FL 32542-5434, to help us maintain a current mailing list.

Do not return copies of this report unless contractual obligations or notice on a specific document requires that it be returned.

REPORT DOCUMENTATION PAGE

Form Approved
OMB No. 0704-0188

1. AGENCY USE ONLY (Leave blank)	2. REPORT DATE	3. REPORT TYPE AND DATES COVERED
	June 1992	Final Mar 91 - Oct 91

4. TITLE AND SUBTITLE

4.5 Micron Laser Source

5. FUNDING NUMBERS

C: F08630-91-C-0006
PE: 63217C
JON: 12020227

6. AUTHOR(S)

Dr M. A. Acharekar and Mr J. Montgomery
Program Manager -- Ron Rapp, WL/MNSI, 882-3160

7. PERFORMING ORGANIZATION NAME(S) AND ADDRESS(ES)

Schwartz Electro-Optics, Inc
3404 North Orange Bloosom Trail
Orlando, Florida 32804

8. PERFORMING ORGANIZATION REPORT NUMBER

9. SPONSORING/MONITORING AGENCY NAME(S) AND ADDRESS(ES)

Wright Laboratory, Armament Directorate
Analysis and Strategic Defense Division (WL/MNS)
Eglin AFB FL 32542-5000

10. SPONSORING/MONITORING AGENCY REPORT NUMBER

WL-TR-92-7016

11. SUPPLEMENTARY NOTES

This report was not edited by WL/MNOI (Scientific & Tech. Info Facility).

12a. DISTRIBUTION/AVAILABILITY STATEMENT

Approved for public release;
distribution is unlimited.

12b. DISTRIBUTION CODE

A

13. ABSTRACT (Maximum 200 words)

This report documents efforts attempted at producing continuous (cw) laser power at 4.5 microns. Silver Galium Selenide (AgGaSe2) was used to frequency double a 9.0 micron CO2 laser. Milliwatts of cw 4.5 micron power were reported. CW damage threshold experiments of AgGaSe2 at 9.0 microns were also conducted.

14. SUBJECT TERMS	15. NUMBER OF PAGES
4.5 Micrometer Laser Frequency Doubled 9.0 CO2 laser Silver Galium Selenide	30 16. PRICE CODE

17. SECURITY CLASSIFICATION OF REPORT	18. SECURITY CLASSIFICATION OF THIS PAGE	19. SECURITY CLASSIFICATION OF ABSTRACT	20. LIMITATION OF ABSTRACT
UNCLASSIFIED	UNCLASSIFIED	UNCLASSIFIED	SAR

PREFACE

This program was conducted by Schwartz Electro-Optics, Inc., Orlando FL 32804 under Contract F08630-91-C-0006 with Wright Laboratory, Armament Directorate, Analysis and Strategic Defense Division, Guidance Navigation and Control Branch (WL/MNSI), Eglin AFB FL 32542-5000. Mr. Ron Rapp, WL/MNSI, managed the program for the Wright Laboratory. The program was conducted during the period from March to October 1991.

TABLE OF CONTENTS

INTRODUCTION

The need for high power or new wavelength lasers has been the motivating factor for the study of Nonlinear Optics for many years. The frequency range of existing lasers can be greatly extended by means of frequency conversion techniques. Of these, second-harmonic generation (SHG), also called frequency doubling, has received considerable attention in comparison to other techniques, including sum frequency mixing (SFM), difference-frequency mixing (DFM) and optical-parametric oscillation (OPO). In addition to these techniques, the Raman cell frequency conversion technique using Stokes and anti-Stokes lines can also extend the primary wavelength of a laser.

SHG has been used to generate coherent radiation ranging in wavelengths from 100 nm out to 2 mm. Of these wavelengths, 4 to 5 microns CW radiation has been an area of interest. By using the second harmonic of the well established CO_2 laser these wavelengths can be obtained. There has been much work in this wavelength range using a pulsed CO_2 laser but very little in CW operation and to our knowledge no work with SHG of 9 μm lasers. In this final report a brief discussion of Nonlinear Optics will be presented with the emphasis on second harmonic generation. Also, the technical approach that was taken will be addressed with results of these experiments given.

NONLINEAR THEORY

When a crystal medium is exposed to an applied electric field, the valence electrons of the medium become displaced forming electric dipoles. The result of the induced dipoles in the medium is the induced polarization (induced dipoles per unit volume). The induced dipoles oscillate at a frequency defined by the combination of the material and incident light. The properties of the reradiated field results from interference of the fields of the induced polarization and the pump beam. If the applied field is weak, then the electrons can follow the changing field. This is the linear case and the induced polarization is proportional to the applied field.

$$P = \epsilon_0 \chi^{(1)} E$$

where ϵ_0 is the permitivity of free space and E is the applied electric field. $\chi^{(1)}$ is the linear optical susceptibility such that $\chi^{(1)} = n^2 - 1$, where n is the linear index of refraction of the medium. Since the radiation is weak the reradiated field is the same as the applied field and no change in frequency is observed.

If the applied electric field is strong (as in a laser) the electrons in the induced dipoles in the crystalline media can not reproduce the applied electric field and induced nonlinear polarization fields. The polarization fields in the media are at a different frequency than the applied field. This over driving of the electrons is what sets up the nonlinear polarization.

To see this more clearly we can expand the induced polarization into higher orders:

$$P = \epsilon_0 [\chi^{(1)}E + \chi^{(2)}E^2 + \chi^{(3)}E^3 + \ldots \chi^{(n)}E^n]$$

with $\chi^{(n)}$ being the n^{th} order nonlinear susceptibility. The effect of $\chi^{(2)}$ is the source term for SHG, SFM, DFM, OPO and more. $\chi^{(3)}$ is the third order nonlinear susceptibility and is responsible for Third Harmonic Generation, two photon absorption, Raman, Brillion and Rayleigh Scattering and four wave mixing.

The nonlinear susceptibility ($\chi(2)_{ijk}$) is a tensor (6X6) quantity with its symmetry dependent on the material. The elements of the tensor define what polarization vectors and propagation direction one must use for a particular nonlinear interaction to take place. Some elements of the tensor may be zero and other will be related. Because of the symmetry restrictions, generally only crystals that do not have an inversion symmetry can be used for second harmonic generation. In nonlinear optics $\chi^{(2)}$ (where the ijk is assumed) is not used but a nonlinear optical susceptibility (d_{ijk}) is defined were $d = \chi^{(2)}/2$. This nonlinear susceptibility tensor d is dependent on both the propagation direction of the pump beam in the crystal medium and the crystal medium itself, making it very complicated expression. A new quantity d_{eff} can be defined that takes the susceptibility tensor elements and the propagation direction into account and gives an "effective" magnitude for the nonlinearity for a given propagation direction. This quantity d_{eff} reduces the tensor to a one-dimensional element simplifying the problem greatly. As an example, the d_{eff} for $AgGaSe_2$ is given as $d_{eff} = d_{36}\sin\theta_{pm}$ for type 1 phase matching and the symmetry class 42m. d_{36} is an element of the susceptibility tensor and is determined experimentally. From the symmetry relations d_{36} is equal to d_{14}. θ_{pm} is the phase matching angle relative to the optical axis. There is a unique d_{eff} for each crystal symmetry class and phase matching type (see Table 1).

All four of the above wave interactions (SHG, SFM, DFG and OPO) must obey the conservation of energy equation

$$\omega_1 \pm \omega_2 = \omega_3$$

where ω_n is the frequency of the interacting waves. In Sum

Frequency Generation (SFM), a nonlinear crystal is pumped by coherent sources with frequencies ω_1 and ω_2 giving the sum frequency of ω_3 (the signal). In this case, $\omega_1 + \omega_2 = \omega_3$ where $\omega_1 < \omega_2 < \omega_3$. SHG is a special case of SFM where $\omega_1 = \omega_2$ or $2\omega_1 = \omega_3$.

Table 1. Effective nonlinear coefficient d_{eff} for selected crystal classes (ref.1)

Crystal class	Two *e* rays and one *o* ray	Two *o* rays and one *e* ray
6 and 4	0	$d_{15} \sin \theta$
622 and 422	0	0
6*mm* and 4*mm*	0	$d_{15} \sin \theta$
$\bar{6}m2$	$d_{22} \cos^2 \theta \cos 3\varphi$	$-d_{22} \cos \theta \sin 3\varphi$
3*m*	$d_{22} \cos^2 \theta \cos 3\varphi$	$d_{15} \sin \theta - d_{22} \cos \theta \sin 3\varphi$
$\bar{6}$	$\cos^2 \theta(d_{11} \sin 3\varphi + d_{22} \cos 3\varphi)$	$\cos \theta(d_{11} \cos 3\varphi - d_{22} \sin 3\varphi)$
3	$\cos^2 \theta(d_{11} \sin 3\varphi + d_{22} \cos 3\varphi)$	$d_{15} \sin \theta + \cos \theta(d_{11} \cos 3\varphi - d_{22} \sin 3\varphi)$
32	$d_{11} \cos^2 \theta \sin 3\varphi$	$d_{11} \cos \theta \cos 3\varphi$
$\bar{4}$	$\sin 2\theta(d_{14} \cos 2\varphi - d_{15} \sin 2\varphi)$	$-\sin \theta(d_{14} \sin 2\varphi + d_{15} \cos 2\varphi)$
$\bar{4}2m$	$d_{14}(\sin 2\theta \cos 2\varphi)$	$-d_{14} \sin \theta \sin 2\varphi$

Since more than one process is possible in a crystal, the conservation of momentum equation

$$k_1 + k_2 = k_3$$

for collinear phase matching

$$n_1/\lambda_1 + n_2/\lambda_2 = n_3/\lambda_3$$

is used to determine which process is dominant where k_n is the wave vector and is equal to $|k| = 2\pi n/\lambda$. For one process to be dominant over another, the phase velocity ($v_p = c/n$) of the interacting waves must be equal. This is known as the phase matching condition and is accomplished by using the crystals birefringence to off-set the dispersion.

SECOND HARMONIC GENERATION

The most important condition for high conversion in three wave mixing is that the process be phase-matched. This insures that the pump and signal are coupled throughout the crystal. In this way the energy flow to the signal is maximum.

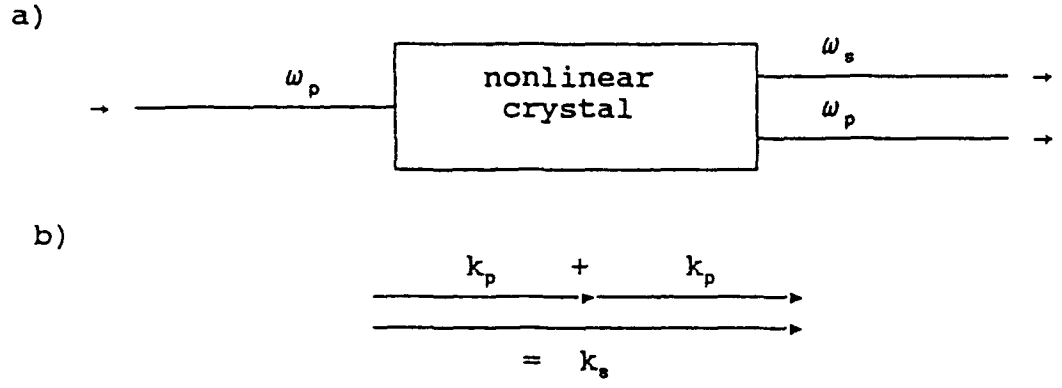

Figure 1. SHG process a) in a nonlinear crystal b) in wave vector space for collinear phasematching.

From Maxwell's equations it is simple to derive the conversion efficiency using the plane-wave low conversion limit[1]

$$\eta = I(2\omega)/I(\omega) = \Gamma^2 L^2 \,\mathrm{sinc}^2 [\Delta kL/2]$$

$$\Gamma^2 L^2 = 2\omega^2 d_{eff}^2 L^2 I(\omega)/n^3 c^3 \epsilon.$$

where d_{eff} is the nonlinearity of the crystal, L is the crystal length, n is the index of refraction of the crystal, c is the speed of light in a vacuum and I is the intensity of the pump (ω) and signal (2ω). $\Delta k = k2\omega + 2k\omega$ is the phase mismatch for SHG. This equation is a good approximation for low conversion efficiencies but does not take into account divergence of the pump beam, pointing vector walk-off, crystal imperfections, absorption, acceptance angle, and spectral acceptance width. All these factors can lead to lower conversion efficiencies.

PHASE MATCHING

In order to achieve phase matching in bulk crystals one uses the birefringence of the nonlinear crystal. For the pump and signal to propagate through the length of the crystal in phase, the indices of refraction for the pump and signal must be equal. One can achieve this by using a uniaxial crystal i.e. a crystal that has two indices of refraction, the extraordinary (n_e) and ordinary (n_o) depending of the polarization and propagation direction. The extraordinary indies can be changed by rotating the crystal with respect to the pump beam by some angle θ with respect to the optics axis (tuning of the extraordinary indices can also accomplished by temperature for some crystals). The amount of change in the extraordinary indices from a rotation θ of the fundamental relative to the optic axis is given by[2]

$$[1/n_e^{2\omega}(\theta)]^2 = (\cos^2\theta)/(n_o^{2\omega})^2 + (\sin^2\theta)/(n_e^{2\omega})^2 .$$

Figures 2 and 3 are graphs of the index of refraction versus wavelength of a negative uniaxial crystal ($n_o > n_e$ for negative, $n_o < n_e$ for positive) for doubling of 1.06 μm. In order for the indices to match, the pump beam (1.064 μm) is input with its polarization along the n_o axis. Therefore, the signal (532 nm) will have its polarization along the n_e axis making the two indices equal for both pump and signal. In most cases (see figure 2), the indices of the two waves are not equal along one of the principle axis, but by rotating the crystal the extraordinary indices can be tuned so that $n_e(\theta)$ of the signal equals n_o of the pump.

In this example the phase matching was type 1 negative because the pump wave propagates with its polarization in the ordinary direction and the signal with its polarization in the extraordinary plane. The types of phase matching are summarized in Table 2 and Figure 4 shows type 1 and 2 phase matching for a negative uniaxial crystal.

Table 2. Phase matching types in uniaxial crystals.

TYPE	NEGATIVE	POSITIVE
I	oo → e	ee → o
IIA	eo → e	oe → o
IIB	oe → e	eo → o

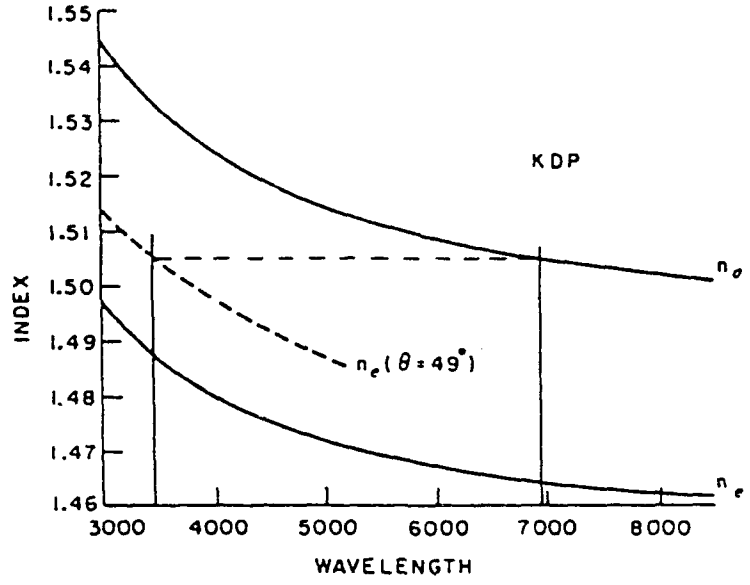

Figure 2. Dispersion curves for KDP crystal showing SHG of a Ruby laser with critical phase matching (ref. 2).

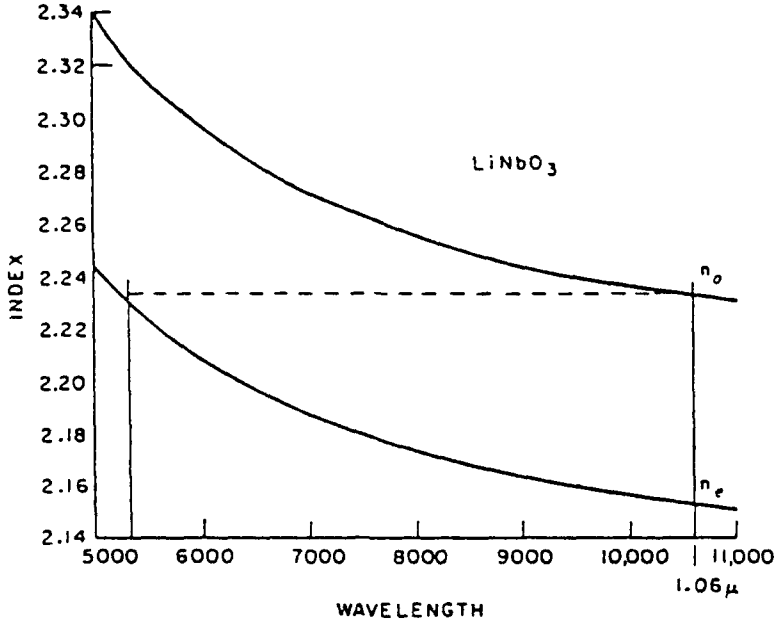

Figure 3. Dispersion curves for LiNbO showing SHG of Nd:YAG laser with noncritical phase matching (ref. 3).

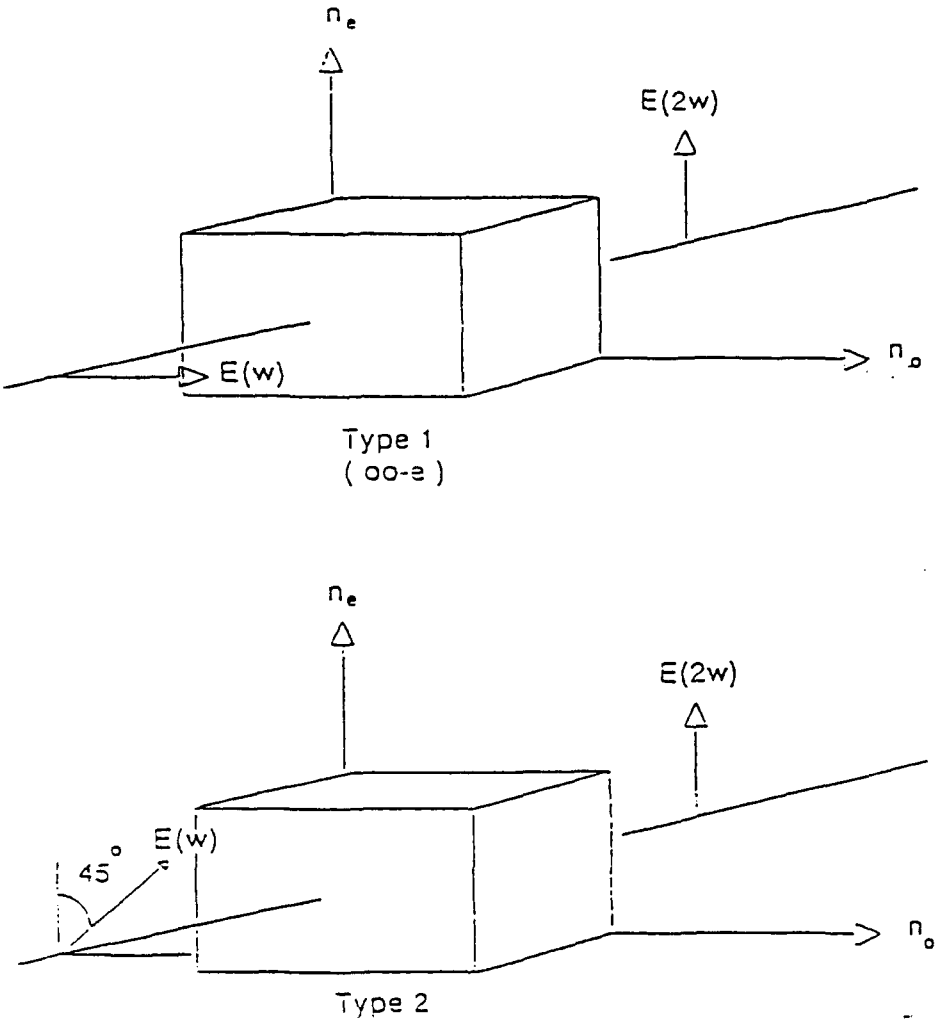

Figure 4. Type 1 and 2 polarization directions for phase matching in negative uniaxial crystals.

A convenient way of determining angles for phase matching is by using the Sellmeier equation[3]

$$n^2(\lambda) = A + B\lambda^2/(\lambda^2 - C) + D\lambda^2/(\lambda^2 - E).$$

The A, B, C, D and E coefficients are determined experimentally and are unique for each crystal type. This equation gives the indices of refraction for the pump and signal frequencies in the ordinary and extraordinary planes. Once this is known the phase matching angle can be calculated by using the equation[4]

$$\sin^2\theta = -\frac{[(n_o^{2\omega})^2/(n_o^{\omega})^2] - 1}{[(n_o^{2\omega})^2/(n_e^{2\omega})^2] - 1}$$

for type 1 phase matching in a negative uniaxial crystal. The Sellmeier coefficients for $AgGaSe_2$ are given in Table 3.

Table 3. Sellmeier coefficients for $AgGaSe_2$ (ref. 5).

	A	B	C	D	E
Ordinary	4.6453	2.2057	0.1879	1.8377	1600
Extraordinary	5.2912	1.3970	0.2845	1.9282	1600

INTRA-CAVITY SHG

Because high power densities are difficult to obtain using a cw laser, the most logical choice is to place the crystal internal to the laser resonator, thereby, taking advantage of the larger power densities and great number of round trips through the nonlinear crystal. If the outcoupling mirror is replaced by a highly reflective mirror at the fundamental and transparent at the harmonic, higher circulating powers can be achieved. The following discussion is a theoretical view of a nonlinear crystal placed intra cavity and the effects on the overall system.

If we assume that the power density inside the resonator is in steady state with the round trip losses equaling the round trip gain then[9],

$$2g_o l/[1 + S/S_o] = L_c + \tfrac{1}{2}KS$$

where

$$g = g_o/[1 + S/S_o]$$

g - gain coefficient
go - small signal gain
S - total fundamental power density in the laser medium
So - saturation parameter
K - nonlinear coupling term
L_c - total round-trip loss at the fundamental except for the loss due to SHG
l - length of the gain medium

The term $\frac{1}{2}KS$ is the loss due to the second harmonic of the fundamental which is transmitted through the outcoupling mirror.

In order to extract useful information from the above equation we will define two normalized quantities α and ξ [10],

$$\alpha = L_c/2g_o l$$

$$\xi = KS_o/4g_o l$$

and

$$K = \Gamma^2 L^2$$

Where α is the normalized loss and is defined as the ratio of the total round trip losses to the round trip unsaturated gain. It is important in determining the available power from the laser as well as the amount of nonlinearity required to extract a given amount of second harmonic power. ξ is the normalized nonlinearity and is given by the ratio of the nonlinear loss to the round trip unsaturated gain for a given fundamental power density.

Figure 5 shows the second harmonic power density S_2 versus the nonlinearity ξ for several values of the loss faction α. From these curves one can see that the second harmonic power increases as the nonlinearity up to a maximum value. For larger values of ξ the SHG output power starts to decrease. Therefore, there is a maximum nonlinearity for a given system and larger

nonlinearities will not help the conversion efficiency. If ξ is maximized it is found that $\xi_{max} = \alpha$ and[11],

$$S_{2max} = g_o l S_o (1 - \sqrt{\alpha})^2 .$$

This equation is plotted in Figure 6 and shows, an important property of intra cavity SHG, that any loss in the resonator not

only reduces the amount of available harmonic power but also the nonlinearity has to be increased in order to extract this power. Therefore, it is very important to reduce all the loss in the cavity to a minimum for maximum available output.

An interesting result of optimum SHG is discovered when examining the nonlinear coupling K. For optimum coupling

$$K = 2L_c/S_o$$

which shows that the second harmonic conversion is proportional to the total loss in the cavity and inversely proportional to the saturation power density but, is not dependent on gain of the laser medium. For a conventional laser system there is only one value for optimum output coupling for a given power level, but, for a system with a intra cavity doubling crystal this optimum condition is met at all power levels.

TECHNICAL APPROACH

INTRODUCTION

From the above discussion two major problems associated with doubling a cw laser can be identified, achieving high enough power densities for high conversion without damage to the nonlinear crystal. In order to resolve these problems associated with cw doubling the following experiments were conducted.

a) $AgGaSe_2$ crystal external to the laser resonator, but use a beam compression scope to increase the power density on the crystal to result in an improved conversion efficiency.

b) $AgGaSe_2$ crystal was mounted on a base which was cooled using a thermo-electric (TE) cooler to maintain the crystal temperature. This will reduce the thermal expansion and avoid crystal damage (cracks).

c) $AgGaSe_2$ crystal placed intra-cavity to improve power density on the crystal to result improved conversion efficiency.

d) $AgGaSe_2$ crystal of type 1 used Brewster angle ends to avoid insertion loss and prevent coating damage.

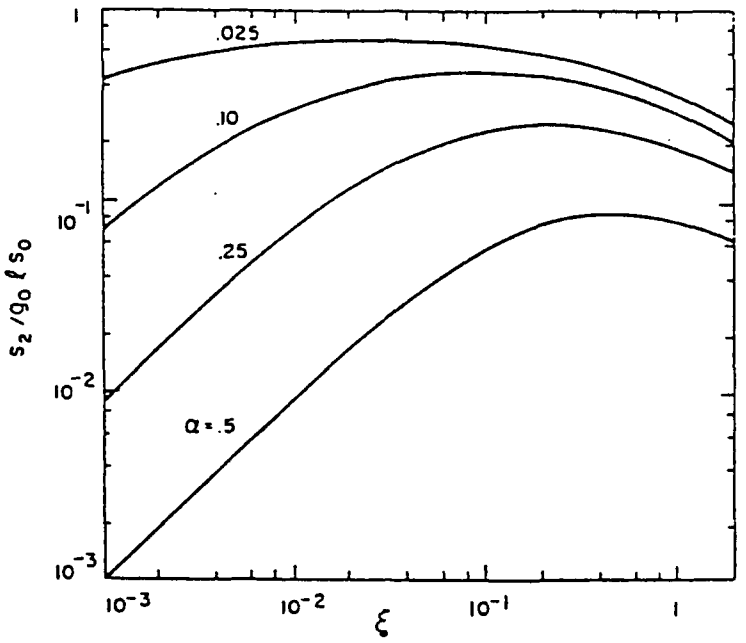

Figure 5. Normalized SHG power density is shown as a function of the nonlinearity ξ for several values of loss fraction α (ref. 9).

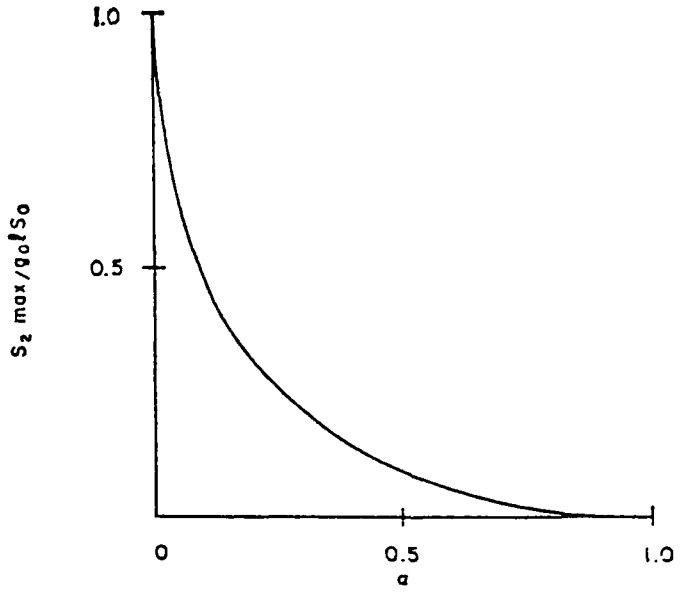

Figure 6. Maximum available SHG is shown as a function of loss fraction α (ref. 9).

$AgGaSe_2$ NONLINEAR CRYSTAL

The CO_2 laser is the main source of laser radiation in the 9 to 11 μm region. Frequency doubling and tripling of the CO_2 laser output produces coherent light in the 2.6 to 5.5 μm region. Table 4 is a list of some of the crystals used for nonlinear interaction in the mid-infrared region. $AgGaS_2$ and CdSe suffer from low figure of merit or low nonlinearity, $AgGaS_2$ has a strong two photon absorption in the 9 to 10 μm region. TAS was found to be a poor choice for doubling of cw radiation due to thermal properties of the crystal. A sample of TAS was borrowed form Dr. Eric Van Stryland at the Center for Research in Electro-Optics and Lasers (CREOL). The piece was place in an unfocused beam at 9 μm at a power of 8 Watts the crystal began to melt at the point of entry of the laser radiation. $CdGeAs_2$ does have a high figure of merit but must be cooled to liquid Nitrogen temperatures to decrease the absorption. The crystal $ZnGeP_2$ has been plagued with growth and absorption problems. The crystal with the highest figure of merit suffers from high linear absorption and because of the large nonlinearity has a very high nonlinear absorption. After considering the tradeoffs $AgGaSe_2$ was chosen for doubling of CW 9 micron laser radiation.

Table 4. Nonlinear crystals for the Infrared (ref. 12).

Material	Transparency Range (μm)	Absorption (cm^{-1} at 10.6 μm)	Damage Threshold (MW/cm^2)	Relative Figure Of Merit (1)
$AgGaS_2$	0.5-13	0.090	15	1.0
CdSe	0.75-20	0.016	50	1.6
$AgGaSe_2$	0.71-18	0.050	12	6.3
TAS	1.26-17	0.040	16	6.5
$CdGeAs_2$	2.4-18	0.230	40	9.2
$ZnGeP_2$	0.74-12	0.900	3	14.0
Te	3.8-32	0.960	45	270.0

(1) The relative figure of merit is based on the value of 14.0 pm/V for SHG at 10.6 μm in $AgGaS_2$.

Table 5. Properties of $AgGaSe_2$ (ref. 13)

Structure type	Chalcopyrite
Crystal symmetry and class	Tetragonal and 42m
Optical transmission (μm)	0.78 to 18.0
Indices of refraction at	n_o n_e
1.064 μm	2.7010 2.6792
4.5 μm	2.6170 2.5850
9.0 μm	2.5990 2.5580
$d\Delta n/dT$ (10^{-6} °C)	~ 1.1
Fresnel reflection loss per surface at 9 μm	18 %
Damage threshold for pulsed (10 ns) at 10.6 μm	25 MW/cm²
Nonlinear Optical Susceptibility (pm/V) for SHG of 10.6 μm	$d_{36} \approx 50$
Phase matching range SHG type 1	3.1 to 12.8 μm
Birefringence Walkoff of 4.5 μm SHG type 1	12 mR
Melting point (°C)	851
Thermal expansion coeff. (10^{-5}/°C)	
$\perp$ to C axis	+ 16.8
$\parallel$ to C axis	- 7.8

$AgGaSe_2$ is a Chalcopyrite crystal[14] which was first proposed in 1972 for nonlinear infrared applications[15]. Early experiments with $AgGaSe_2$ demonstrated its potential[16]. However, it was beset with crystal growth difficulties. The growth related problems of $AgGaS_2$ and $AgGaSe_2$ are similar, and experience gained with previous growth of the sulfide was directly applicable to the selenide. Both materials are volatile at their melting temperatures and must be grown in sealed ampoules using the Bridgeman-Stockbarger technique. Both have anomalous expansion along c axis. Therefore, it is necessary to seed the boule in the c direction and to use precision tapered ampoules to avoid cracking when cooling after growth. Large crystals can only be grown with nonstoichiometric composition which result in finely dispersed scattering centers. Post growth

heat treatment in the presence of access Ag_2Se in the case of $AgGaSe_2$ is then required to remove the scattering centers[17]. Recently, Cleveland Crystals, Inc., (CCI) Cleveland, Ohio started manufacturing and commercially marketing these crystals. The data provided in this paper were collected using crystals manufactured and supplied by CCI. CCI provided crystals of size 8 mm diameter by 5, 10, 20 mm long, and a 5 mm diameter by 20 mm. In addition, 5 mm diameter by 1 mm thick samples were provided for the damage measurements.

There is a significant body of work published on second harmonic conversion of pulsed CO_2 laser radiation and the laser damage threshold of the SHG crystals[18,19]. A brief review of the important work is provided in this section. A CO_2 transversely excited atmospheric (TEA) laser was selected by R. C. Eckardt et. al.[20] Using a 20 mm long $AgGaSe_2$ crystal 14 percent (%) energy and 60 % peak intensity conversion efficiency was demonstrated. It was reported that the conversion efficiency in the crystal was limited by surface damage which occurred at 12 MW/cm^2 peak intensity or energy fluence of 3 J/cm^2 for the TEA laser pulse. A more recent work[21] indicates that for a continuous wave (CW) CO_2 laser, the second harmonic conversion efficiency and the material damage threshold are both very low. The average damage threshold of the coated surface was 4.85 +/- 1.81 kW/cm^2 and the minimum threshold for damage was 2.5 kW/cm^2. This low surface damage threshold creates a serious problem for obtaining high SHG conversion efficiency since, the conversion efficiency depends on the input laser power density.

The experimental data obtained for pulsed CO_2 laser showing high conversion efficiency is shown in Figure 7. The theoretical efficiency calculations were performed at low power densities of a CW laser. This theoretical data are shown in Figure 8 and where calculated using the efficiency equation in the Second Harmonic Generation section. It is clear that due to the low damage threshold (approximately 5 kW/cm^2) for $AgGaSe_2$ using CW laser, only 0.06 % conversion efficiency can be obtained. Thus, for a CW laser providing 10 W power when focused in a crystal resulting less than 5 kW/cm^2 power density will result a maximum of 6 mW frequency doubled output. Therefore, the increase in the surface damage threshold of $AgGaSe_2$ is important.

Thus, in summary, there are two basic problems associated with frequency doubling CW CO_2 laser using $AgGaSe_2$ crystal: (a) low laser damage threshold of the crystal, (b) poor conversion efficiency at low input power density.

The damage of $AgGaSe_2$ can be characterized in two ways 1). Macroscopic damage 2). Microscopic damage mechanisms. The thermal properties of $AgGaSe_2$ are such that when heated the crystal expands in the a and b crystal graphic directions but contracts in the c direction. This sets up stresses in the crystal lattice that

led to very small micro cracks. The micro cracks form absorption centers that progress into damage. After many thermal cycles the cracks begin to grow. A $AgGaSe_2$ crystal 10 mm and 5 mm radius had these cracks in one third of the crystal.

Micorscopicly, a crystal can be thought of as a plasma with the ions in the crystal lattice and the electrons dispersed throughout the solid. If the incident radiation has a frequency near the ion acoustic frequency then this cause a parametric interaction with the electrons causing absorption of the pump radiation. This heating cause the damage to the crystal. This effect is known as a parametric instability and explains the low damage threshold of semiconductor materials from 10.6 μm cw radiation[21].

LASER DAMAGE THRESHOLD

For laser damage threshold measurements of $AgGaSe_2$ crystal surface coated for anti-reflection (AR) at 9 micron was used. The samples were 1 millimeter thick, 5 millimeters in diameter with AR coatings on both surfaces. The AR coating were standard high temperature coatings. The makeup of the coatings were considered company prioritary and were not discussed with SEO.

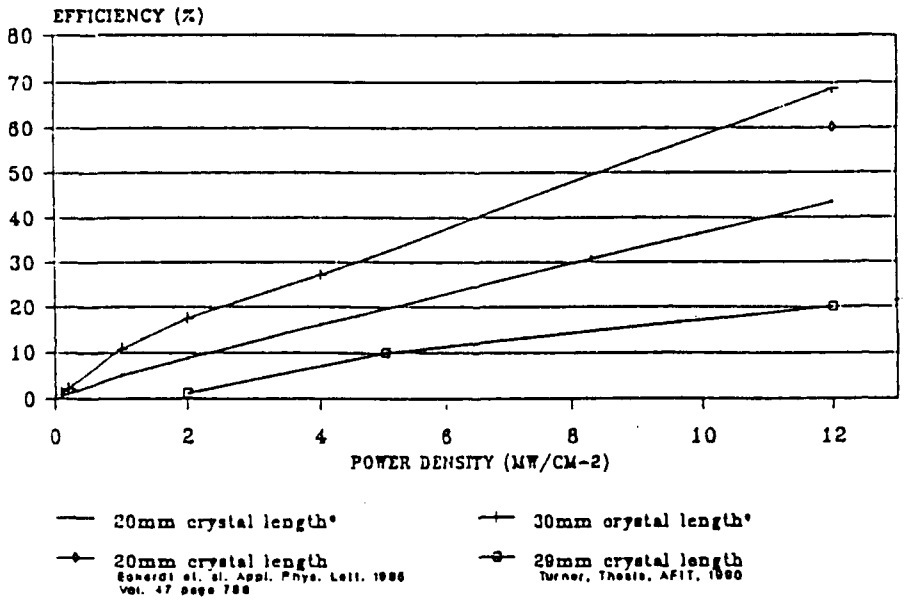

Figure 7. High power conversion efficiency using $AgGaSe_2$.

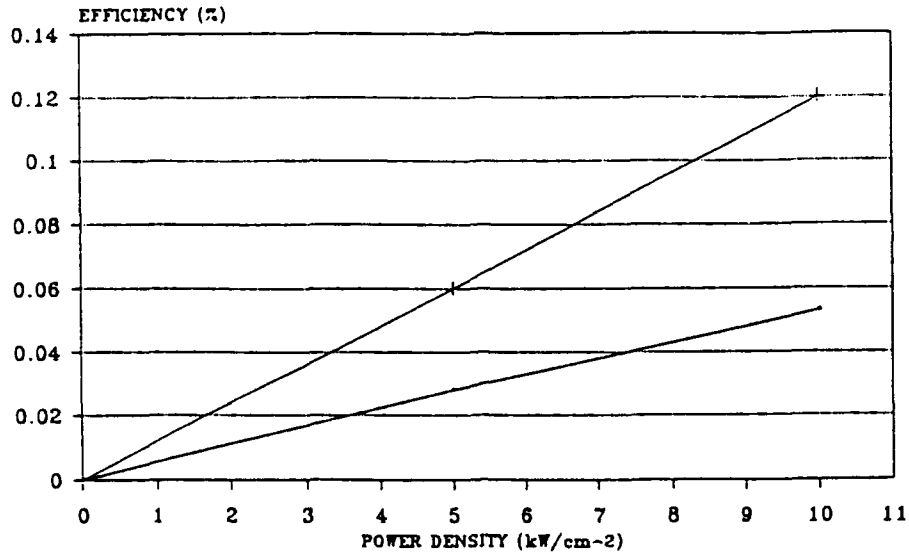

Figure 8. Low power or CW conversion efficiency using $AgGaSe_2$.

The experimental schematic is shown in Figure 9. The lens is Zinc Selinide with AR coatings. The samples were mounted in a copper holder which attached to a Thermo-electric (TE) cooler. The TE cooler is placed on a heat sink that is cooled by water flow. The temperature can be varied form - 20 degrees celsius to room temperature. A nitrogen flow was used below 10 degrees C to prevent water from condensing on the surfaces. A beam spliter was used to monitor the input power. The power was measured using a Coherent Labmaster-E with ether the L-10 or L-100 detector heads for low and high power respectively.

A Ultra Lasertech model PX2500GLS sealed off CW CO_2 laser operating between 9.042 microns and 9.42 microns was used. All damage measurements were conducted using the 9.042 wavelength (R36 line). The laser was operated with a single TMoo mode. The beam divergence of 2.5 mR.

The front surface of the $AgGaSe_2$ samples were placed at the focal plane of the 1.5 inch lens. As the power was increased the damage was detected visually. Table 6 shows the damage thresholds for two conventional AR coating obtained form different sources. Each power level irradiating the crystal sample was sustained for at minimum of 5 minutes before moving to a higher level. Damage always occurred upon irradiation of the sample. The damage did not seem to be dependent on the amount of time the sample was exposed. The damage was a single pit with traces of silver lining the sides.

In some cases, the entire sample was fractured from one damage site. Two samples were used for the CCI damage testing with two damage sites on one and one on the other because it fractured with just one damage spot. Damage data is as follows 23.4 18.0 and 22 kW/cm^2. The LOC damage was done with one sample and two damage sites. The coatings began to flake before more damage testing could be conducted. The damage data was 60 and 59 kW/cm^2. Figure 10 shows the reflectance of the AR coating done by Lightning Optical Corp. between 4 and 10 μm.

The samples were tested for damage at room temperature and at 0 degrees Celsius. There was no significant change in the damage threshold due to the lowering of the temperature.

FREQUENCY DOUBLING EXPERIMENTS

In order to resolve the problems noted in section 1, associated with $AgGaSe_2$ crystal used with a CW CO_2 laser the following experiments were conducted:

a) $AgGaSe_2$ crystal external to the laser resonator, but use beam compression scope to increase the power density on the crystal to improve conversion efficiency.

b) $AgGaSe_2$ crystal was mounted on a base which is cooled by using a thermo-electric (TE) cooler to maintain the crystal temperature.

c) $AgGaSe_2$ crystal was placed intra-cavity to improve power density on the crystal to improve conversion efficiency.

d) $AgGaSe_2$ crystal type 1, is Brewster angle cut at both ends to avoid insertion loss and prevent coating damage.

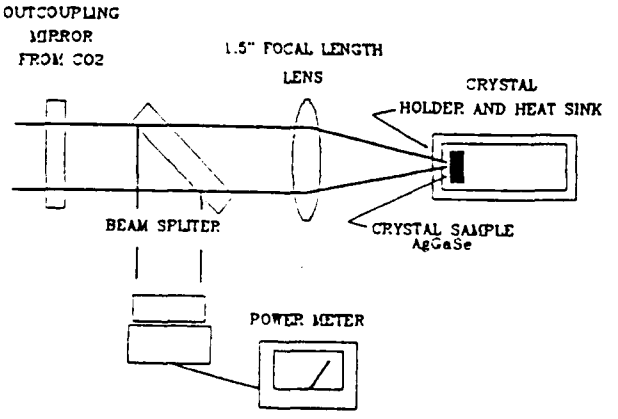

Figure 9. Experimental setup for damage threshold measurements.

Table 6. Surface damage threshold of $AgGaSe_2$ for CW CO_2 laser.

No.	AR coating By	Reflection Loss Per Surface	Average Damage Threshold	Reference
1	CCI	8.5 percent	22 kW/cm²	This Work
2	LOC	2.0 percent	60 kW/cm²	This Work
3	CCI	Not Known	5 kW/cm²	Ref. 9
4	Uncoated	20 Percent	10 kW/cm²	Ref. 9

AR coating manufacturer's code:
CCI - Cleveland Crystals, Inc.
LOC - Lightning Optical, Corp.

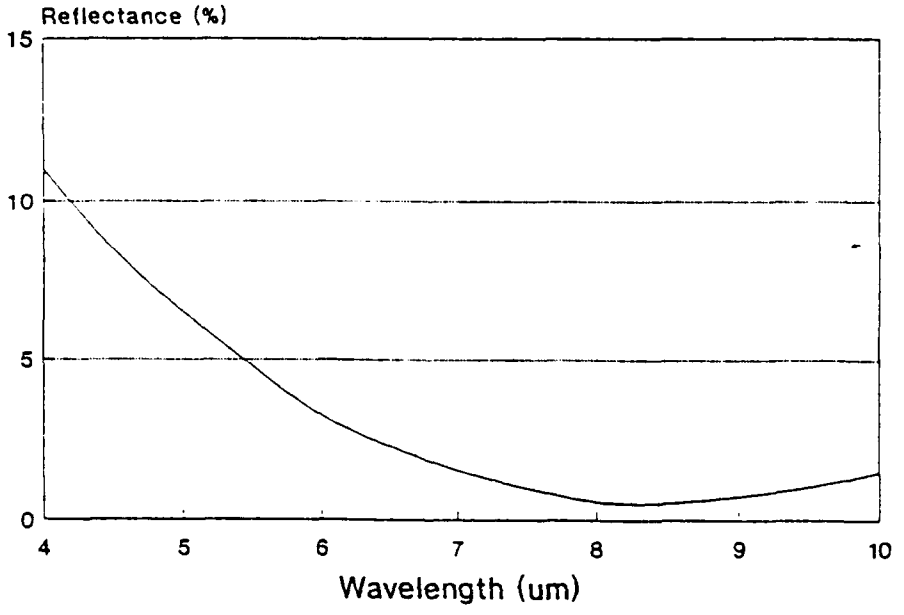

Figure 10. AR coatings for $AgGaSe_2$ coated by Lightning Optical Inc.

Below is a brief discussion of the above four experiments.

1. External $AgGaSe_2$ Crystal using Compression Optics

An $AgGaSe_2$ crystal 2 centimeters in length and 8 millimeters in diameter was placed external to the resonator with a 3X compression scope between the crystal and the laser (see Figure 11). The spot diameter before the scope was 4 mm ($1/e^2$) and after was compressed to 1.3 mm, thereby increasing the power density inside the crystal. The power density with 10 Watts pump power is approximately 1.4 kW/cm^2 corresponding to a theoretical conversion efficiency of 0.01 % which predicts an output at 4.5 microns of 1 mW. The measured output at 4.5 microns was 50 microWatts. The theoretical conversion equation predicts some what higher numbers due to the plane wave approximation and not taking into account the crystal parameters such as beam walk off, angular and frequency acceptance bandwidth. The lower conversion efficiency is therefore not unexpected. Figure 12 shows the polarization directions for the pump (9 μm) and signal (4.5 μm) beams for the $AgGaSe_2$ crystal.

A calibrated Eltec pyro-electric detector was used for the power measurements with a chopper at 2.5 kHz. The detector was calibrated using a He-Ne 10 mW cw laser. Because of the very flat spectral response of the pyro-electric detectors (from 200nm to 30 μm), the calibration was one to one for the wavelengths involved. The chopper was used because a pyro-electric detector needs a pulsed input. The chopping frequency was held constant throughout the experiment.

The phase matching angle of $AgGaSe_2$ for a given wavelength is plotted in Figure 13 for two different crystals. The crystals were cut for doubling of 9 micron at an internal angle of 47.3 degrees. This angle was chose to be the angle at which the beam propagated at normal incidence to the crystal face. It can be seen that these crystals are not cut for phase matching at 9 microns. This is due to the inaccuracies of the Sellmeiers coefficients and / or errors in cutting the crystal.

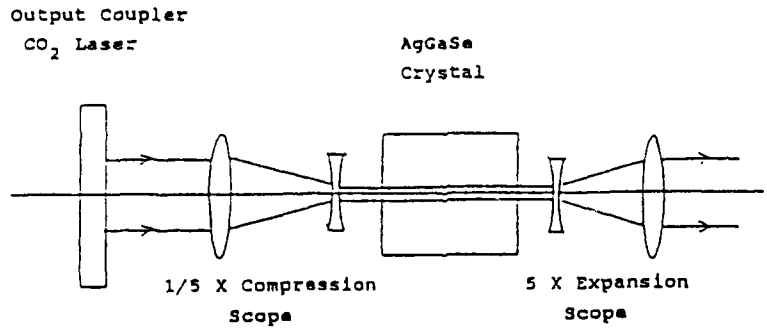

Figure 11. External SHG using compression optics.

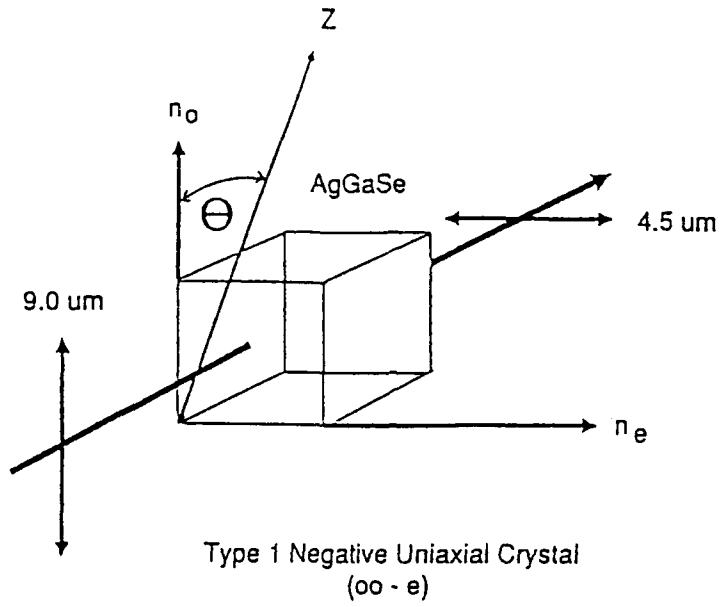

Figure 12. Polarization direction for SHG of 9 μm.

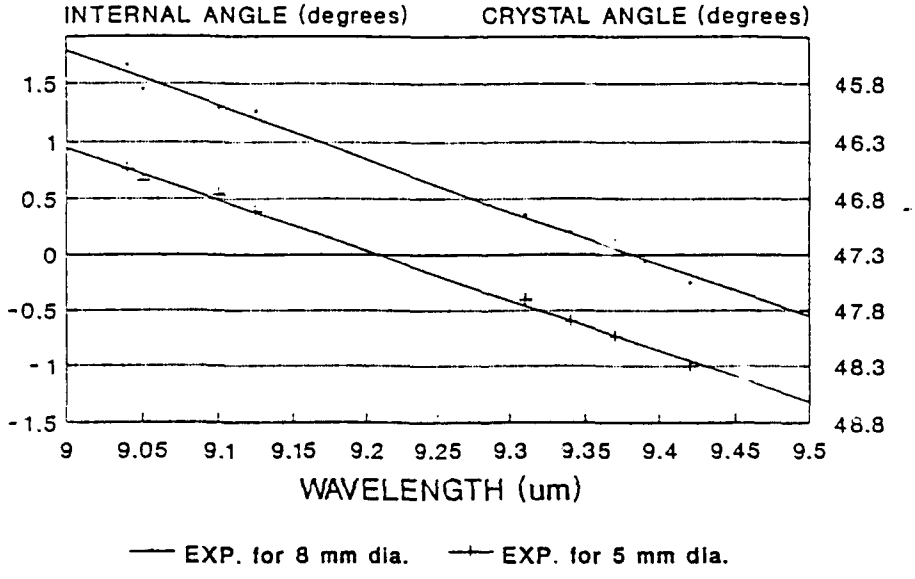

Figure 13. Experimental phase matching angles for two different pieces of $AgGaSe_2$.

2) TE Cooler For $AgGaSe_2$ Crystal

This experiment evaluated the effects of lower temperature on the damage threshold and phase matching of the crystal. The damage threshold reported (ref. 13) for 10 ns pulsed laser operating at 10.6 microns is 20 MW/cm^2. It may be noted that the mechanisms of damage in pulsed and CW lasers are different. The damage mechanism in $AgGaSe_2$ crystal with a CW laser will be initial thermal cracks and then absorption of laser power resulting in optical damage. Therefore, it was hoped that the TE cooler maintaining lower crystal temperatures (typically 10 °C or lower) would solve the thermal problems. As mentioned earlier this approach had little effect on the damage threshold of $AgGaSe_2$. Also, the temperature was varied from 0 °C to 40 °C with no appreciable change in the output at 4.5 microns. This was expected because of the phase matching angle insensitivity of $AgGaSe_2$ to temperature (see Table 5, $d\Delta n/dT$).

3) Intra-Cavity $AgGaSe_2$ Crystal

The output coupler was removed form the laser and replaced with a window coated with anti-reflection (AR) coating for 9 micron and maximum reflection for 4.5 micron on the second surface. The second mirror coated for maximum reflectivity for 9 micron on one surface and AR coating for 4.5 micron on the second surface was mounted external to the discharge tube (see Figure 14). An $AgGaSe_2$ crystal was mounted in between these two mirrors, thus, only the output frequency doubled will be extracted out of the laser resonator. This provided improved conversion efficiency due to the higher circulating power and increased number of round trips of the 9 micron in the cavity ie the crystal.

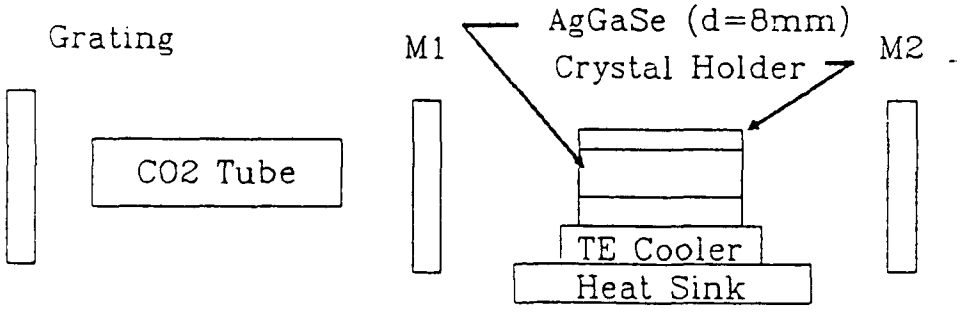

M1 HR at 4.5um, HT at 9um
M2 HT at 4.5um, HR at 9um

Figure 14. Schematic of SHG intra-cavity.

A 3X compression scope was added for increased power density in the crystal. Using the 20 mm long, 8 mm diameter crystal with the 3X compression scope, an output at 4.5 micron of 2.5 mW was detected using a calibrated pyro-electric detector. The wavelength of the laser was changed to 9.4 microns to take advantage of the higher gain and phase match at an angle closer to normal incidence. An output power of 4 mW was observed at 4.7 microns. No damage to the crystal was observed.

4) Brewster Angle on the $AgGaSe_2$ Crystal Ends

In this experiment the $AgGaSe_2$ crystal was cut with its Type 1, angle of 47.3 degrees for 9 microns, and the ends of the crystal were cut at Brewster's angle. Brewsters angle cuts eliminate the need for AR coatings on the crystal ends. The reflection loss with brewster ends is generally much lower than the AR coatings. Secondly, the damage problems associated with dielectric coatings are also eliminated. Figure 15 shows a Brewsters angle cut crystal with both the phase matching and Brewsters angle conditions met, where[22]

$$\theta_B = \tan^{-1}(n)$$

$$\theta_R = \sin^{-1}[\sin\theta_B/n]$$

$$\theta_2 = \pi/2 - \theta_R$$

$$\theta_1 = \theta_M - \theta_2.$$

It can be seen from Figure 15 that because the fundamental and signal are orthoganally polarized that there will be losses at the signal due to the Brewster face cut for the fundamental. Also, Brewsters angle cut SHG will only work for type 1 phase matching. For intra-cavity SHG the loss at the fundamental is more important than the loss at the signal therefore, Brewsters angle cut nonlinear crystals are commonly used for intra-cavity experiments.

Because of the reduced aperture from cutting a 8 mm diameter crystal near Brewster's angle and tilting the crystal, the crystal acted like a iris in the cavity cutting the circulating power. For this reason and the fact that the brewster angle presents a loss at 4.5 μm, the experiments did not do as well as the normal cut crystals. Maximum output at 4.5 μm was 1 mW. It is believed that if a larger diameter crystal is used the brewster cut crystal will outperform the normal cut crystals.

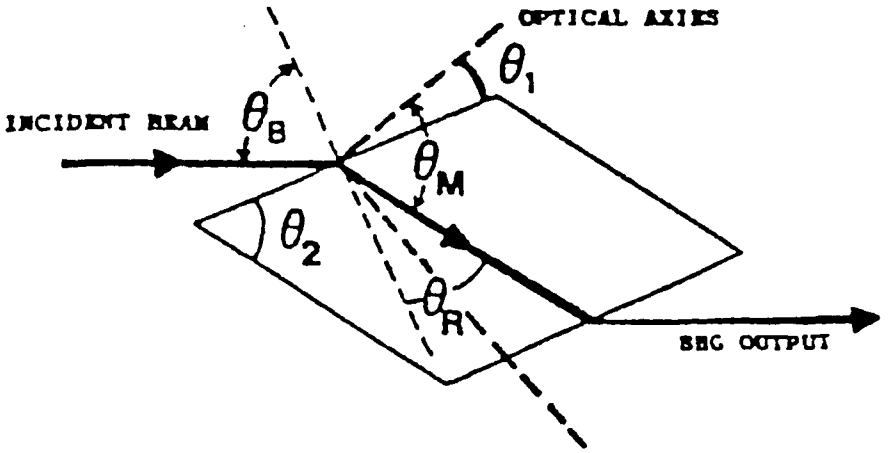

Figure 15. SHG Brewsters angle cut crystal phase matching angle and Brewsters angle condition (ref. 23).

SUMMARY

(a) For the use of $AgGaSe_2$ in CW lasers, there are two basic issues which must be addressed: (i) low laser power density in the crystal and (ii) low laser damage threshold.

(b) The laser power density in the doubling crystal was increased by placing the crystal intra-cavity and by using beam compression optics.

(c) The relatively high index of refraction causes significant insertion loss (20 percent per surface). Therefore, AR coating was used on the crystal ends. The insertion loss was reduced to 2 percent per surface. Also, a crystal with ends cut at a Brewster's angle was used in the experiments.

(d) The laser damage threshold was measured for the AR coated $AgGaSe_2$ crystal surfaces. The damage threshold, as well as the insertion loss, was improved by a factor of three or more.

(e) The samples used for damage threshold were mounted in a copper block and cooled using a TE cooler. The temperature of the sample under test was changed from -20 to 20 °C and damage threshold measurements were performed at -20, -10, 0, 10 and 20 °C. There was no significant difference in the surface damage threshold at different temperatures.

(f) The damage mechanism appears to be thermal in nature and the entire crystal shows fractures around the surface damage spot.

(g) In spite of improved surface damage threshold of the AR coated crystal ends, a poor conversion efficiency was observed. This low doubling efficiency was due to the internal quality (bulk damage) of the crystals used for the experiments.

ACKNOWLEDGEMENT

This work was conducted under Contract No. F08630-C0006 from the Department of the Air Force, Wright Laboratory, Eglin Air Force Base, Florida.

REFERENCES

1. F. Zernike and J.E. Midwinter, APPLIED NONLINEAR OPTICS, (John Wiley and Sons N.Y.,1973), p. 64 - 66.

2. R.L. Byer, Nonlinear Optics, edited by P.G. Harper and B.S. Wherratt, (Academic Press, N.Y., 1977), p. 64.

3. R.L. Byer, Nonlinear Optics, edited by P.G. Harper and B.S. Wherratt, (Academic Press, N.Y., 1977), p. 65.

4. D. Hon, Laser Handbook Vol. 3, (North-Holland Publishing Co., 1979), p. 425.

5. A. Yariv and P. Yeh, Optical Waves in Crystals, (John Wiley and Sons, 1984), p. 523.

6. H. Kildal and J.C. Mikkelsen, Optics Comm., Vol. 9, p. 317, 1973.

7. D. Hon, Laser Handbook Vol. 3, (North-Holland Publishing Co., 1979), p. 421.

8. N. Barnes and K. Murray, Advanced Solid-State Lasers, edited by H.P. Jensssen and G. Dube, Vol. 6, p. 322, 1990.

9. R.G. Smith, J. Quantum Electron., Vol. QE-6, p. 216, 1970.

10. R.G. Smith, J. Quantum Electron., Vol. QE-6, p. 216, 1970.

11. R.G. Smith, J. Quantum Electron., Vol. QE-6, p. 216, 1970.

12. J.T. Lin and C. Chen, Laser and Optronics, Nov. 1987, p. 59.

13. Silver Gallium Selenide and Silver Gallium Sulfide, Information Sheet, Cleveland Crystal, Inc., Cleveland, OH., January 1990.

14. R. L. Byer, M. M. Choy, R. L. Herbst, D. S. Chelma, and R. S. Feiglson, Appl. Phys. Lett., vol. 26, p. 224, 1987.

15. G. D. Boyd, H. M. Kasper, J. H. McFee, and F. G. Stortz, IEEE J. Quantum Electron, vol. QE-8, p. 900, 1972.

16. H. Kildal, and J. C. Mikkelsen, Opt. Commun., vol. 9, pp. 315-318, 1973.

17. R. K. Route, R. S. Feigelson, R. J. Raymakers, and M. M. Choy, J. Cryst. Growth, vol. 33, p. 239, 1976.

18. D. C. Hanna, B. Luther-Davies, H. N. Rutt, R. C. Smith, and C. R. Bradley, IEEE J. Quant. Electron. vol. QE-8, p. 317, 1972.

19. J. C. Mikkelson, and H. Kildal, J. Appl. Phys., vol. 49, pp. 426-431, 1978

20. R. C. Eckardt, Y. X. Fan, R. L. Byer, R. K. Route, R. S. Feigelson, and Jan Van der Laan, Appl. Phys. Lett. vol. 47, pp. 786-788, 1985

21. M. D. Turner, "Characterization of $AgGaSe_2$ and $ZnGeP_2$ for frequency doubling CO_2 laser output," Thesis for Master of science in Engineering Physics, Air Force Institute of Technology, AFIT/ENG1GEP/90D, 1990.

22. S.K. Gulati and W.W. Grannemann, Boulder Damage Sysmposium, page 357, 1976.

23. J.T. Lin, Proceedings of International Conference on Lasers '86, p. 262, 1986.

DISTRIBUTION

Defense Technical Info. Center DTIC-DDAC Cameron Station Alexandria VA 22304-6145	2
AUL/LSE Maxwell AFB AL 36112-5564	1
AFCSA/SAMI Pentagon, Room 1D363 Washington DC 20330-5425	1
SDIO/TNS Attn: Cmdr Korejwo The Pentagon Washington DC 20301-7100	1
WL/MN Eglin AFB FL 32542	1
WL/MNSI Eglin AFB FL 32542	4
WL/MNOI Eglin AFB FL 32542	1
WL/CA-N Eglin AFB FL 32542	1